Results and discussion

Abrogation of p53 by the introduction of the HPV16-E6 gene

One of the main objectives of this study was to determine the cellular responses to DNA damage when the G2-phase checkpoint was abrogated in the presence or absence of the p53 tumor suppressor under isogenic conditions. For this purpose, we adopted an established method to abrogate p53, i.e., the introduction of the E6 gene of human papillomavirus type 16 (HPV16) [14,20]. The HPV16 E6 gene was transfected into the human lung adenocarcinoma cell line A549, which has functionally active p53, to derive the p53-deficient cell line A549-E6. E6 gene expression was confirmed in the A549-E6 cells by RT-PCR (data not shown). As a control, the A549-neo cell line was established by transfecting A549 with the original vector, which contained a gene for neomycin resistance.

As indicated in Fig. 1A, the A549-E6 cells contained neither stabilized p53 nor induced levels of p21, which is a p53-regulated CDK inhibitor [17,21], following adriamycin treatment. The abrogation of p53 in A549-E6 cells was also seen in the luciferase assays. There was no induction of luciferase activity following adriamycin treatment of cells that were transfected with luciferase reporter plasmids, such as PG13, which contains a tandem array of p53-binding sequences [16], and pWWP, which contains p53-binding sites in the 5′-untranslated region of the p21 gene ([17]; data not shown).

In order to synchronize the cells at the G2 phase, they were treated with 2.5 mM aphidicolin for 24 h and then treated with 100 ng/ml adriamycin for 15 h because a single shot of adriamycin induces G1 arrest in A549-neo cells [14]. This two-step synchronization enriched the G2 cell populations of both cell lines. (Data are not shown. See Fig. 2B at Time 0.) In contrast to what was seen with adriamycin treatment, the addition of aphidicolin to A549-neo cells led to weak stabilization of p53 and slight induction of p21, but this drug had little effect on cell cycle progression when the cells were released from the blockade. Stabilization of p53 and induction of p21 were observed only in two-step-synchronized A549-neo cells, and not in A549-E6 cells (Fig. 1B).

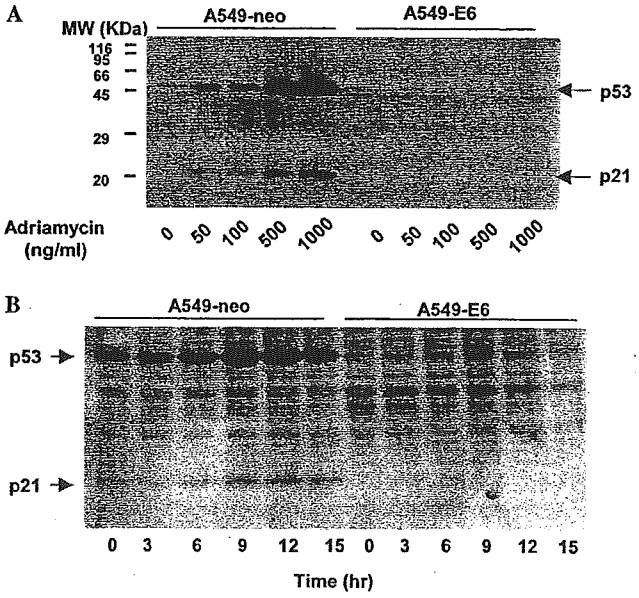

Fig. 1. Loss of p53 function in HPV16 E6-transfected cells. A549 human lung adenocarcinoma cell lines were established that carried either a control neomycin-resistant vector (A549-neo) or a vector that contained the E6 gene of HPV16 (A549-E6). (A) The logarithmically growing cells were treated with the indicated concentrations of adriamycin for 24 h. Cell extracts were prepared and the expression levels of p53 and p21 were analyzed by Western blotting. The p53 and p21 signals are indicated with arrows. (B) The p53 and p21 proteins were analyzed at 3-h intervals after release from aphidicolin treatment in the presence of 100 ng/ml adriamycin. Protein samples (25 μg per lane) were analyzed by Western blotting in A and B.

Slower M phase traverse in A549-E6 cells after the abrogation of G2 arrest by caffeine

Caffeine treatment of G2-arrested, DNA-damaged cells induced mitotic catastrophe and apoptosis in p53-null cells [22] through the inhibition of ATM and ATR kinase activities [23,24]. In the present study, somewhat different phenotypes were observed for the caffeine-treated A549-neo and A549-E6 cells (Figs. 2A and B). As shown in Fig. 2A, some round cells were observed 3 h after the addition of caffeine to the A549-neo cells, and most of the G2-arrested cells contained G1 DNA content at 9 h posttreatment. On the other hand, the A549-E6 cells started to round at 3 h in a manner similar to that of the wild-type cells, but the round cells accumulated until 9 h posttreatment. After 12 h, a subpopulation that consisted of two round cells that were attached to each other increased. Cells of this type persisted at 15 h, at which time most of the wild-type A549-neo cells had completed the M phase of growth. Flow cytometric analysis of A549-E6 cells (Fig. 2B) gave similar results. However, some differences were discerned during the morphological analysis. Microscopic examination of the A549-E6 cells at 12 and 15 h posttreatment revealed a relatively high frequency of two round cells attached to each other, even though flow cytometry indicated that most of these cells had G1 DNA contents. We suspected that the doublet cells, which were probably in a telophase-like state, were mechanically separated during sample preparation for flow cytometry. Despite this minor problem, it was evident that cells that contained integrated E6 and that were p53-deficient behaved differently than wild-type A549 cells in terms of M-phase progression, presumably completing mitosis, when the G2-phase checkpoint was abrogated.

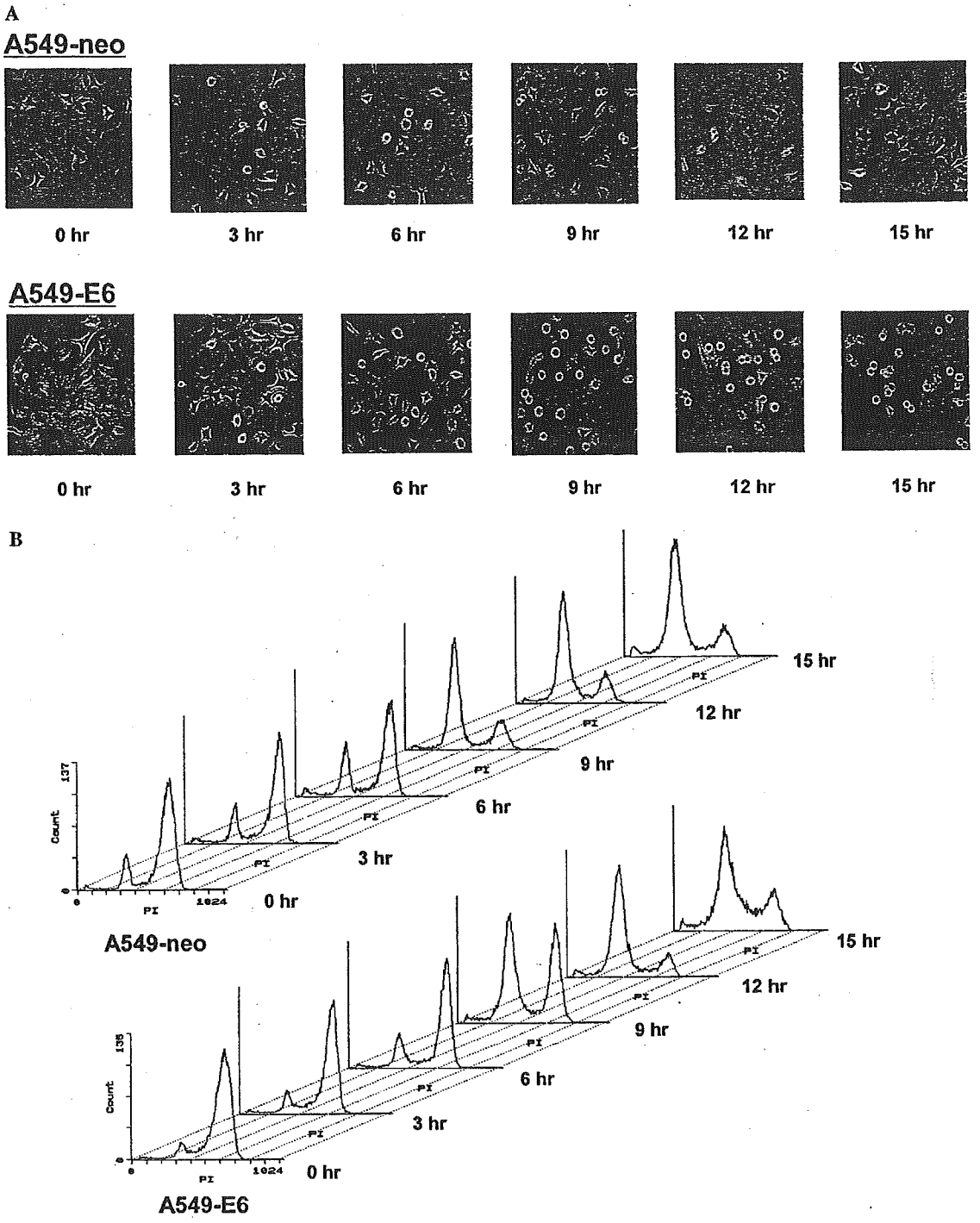

Fig. 2. Microscopic and flow-cytometric analyses of A549-neo and A549-E6 cells after treatment with caffeine. Cells were treated with aphidicolin to synchronize at early S phase followed by adriamycin in order to trap cells at the G2 phase. Such cells were treated with caffeine to abrogate G2-phase arrest. (A) Microscopic views of A549-neo and A549-E6 cells every 3 h after the addition of 2.5 mM caffeine to G2-phase-synchronized cells. (B) Cell cycle distribution determined by flow cytometric analysis of A549-neo and A549-E6 cells every 3 h after the addition of caffeine to G2-arrested cells.

Higher CDK activity in A549-E6 cells than in A549-neo cells

To explain the phenotypic differences in M-phase traverse between A549-neo and A549-E6 cells after treatment with caffeine, we measured the CDK1 and CDK2 activities, since the levels of these enzymes correlate with M-phase progression.

Fig. 3A shows the kinetics of CDK1 activity in G2-arrested cells after treatment with caffeine. The kinase

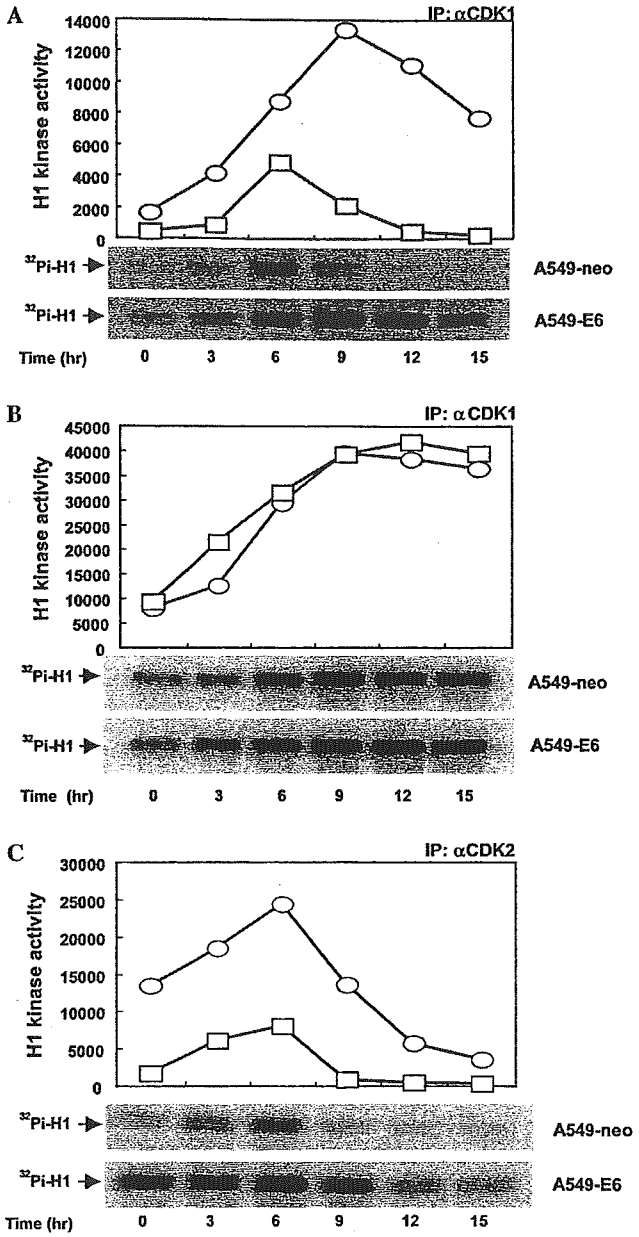

Fig. 3. Changes in the histone H1 kinase activities of CDK1 and CDK2 after the addition of caffeine to G2-arrested cells. (A) CDK1 activity of immunoprecipitates from caffeine-treated, G2-arrested A549-neo and A549-E6 cells was monitored at 3-h intervals. Images of the phosphorylated histone H1 are shown in the lower panels, and the protein levels are quantified and plotted in the upper panel. The rectangles denote values for the A549-neo cells, and circles represent the values for the A549-E6 cells. (B) The CDK1 activities in cells from A that were treated with 100 nM nocodazole and 2.5 mM caffeine. The upper panel indicates the quantitative analysis of the CDK1 activities shown in the lower panels. The symbols are the same as those in A. (C) CDK2 activity is shown as in A and B and the symbols are the same as those in A. Experiments in A, B, and C were conducted more than three times and the typical results are shown.

activity of A549-E6 cells increased for the first 9 h after the addition of caffeine and then gradually decreased, but high CDK1 activity was still detected. The kinase activity patterns of caffeine-treated A549-neo cells were clearly different (Fig. 3A). First, CDK1 activity after caffeine treatment was much lower in A549-neo cells than in A549-E6 cells at every time point. Second, the CDK1 activity of A549-neo cells returned to the basal level at 12 h, at which time point the A549-E6 cells still had high-level kinase activity. Although the maximum CDK1 activity was relatively low, flow cytometric analysis indicated that the A549-neo cells passed through the M phase (Fig. 2B). These results suggest that A549-neo cells exit the M phase more quickly than A549-E6 cells; this may reflect the lower frequency of round cells during caffeine treatment. To confirm this hypothesis, we used nocodazole to trap cells at pseudo-metaphase. The combined application of nocodazole and caffeine (Fig. 3B) activated CDK1 to similar levels in both cell types. This finding suggests that a factor that suppresses CDK1 overactivation is present in A549-neo cells but absent in A549-E6 cells. We also examined the kinetics of CDK2 activation following treatment with caffeine. Essentially, the same activation profiles were observed in A549-neo and A549-E6 cells, i.e., CDK2 activity increased up to 6 h after the addition of caffeine and decreased thereafter (Fig. 3C). Nevertheless, there were obvious differences in the levels of CDK2 activity. The basal activity of CDK2 was remarkably higher in A549-E6 cells than in the wild-type cells. This result was reflected in the levels of CDK2 activity measured at 6 h, when CDK2 activity was maximal in both cell lines.

Stable cyclin B1 in caffeine-treated A549-E6 cells

In order to examine further the different phenotypes of the two cell lines, we assayed proteins that were related to CDK1 and CDK2 in the G2 to M phases by Western blotting (Fig. 4).

The p53 and p21 proteins were detected only in A549-neo cells and were abrogated by the introduction of the E6 gene (see also Fig. 1B). Three CDK1-specific bands were detected for up to 6 h. The two upper bands, which represented the inactive phosphorylated forms of CDK1, decreased after 6 h. These results correlate well with the kinetics of activation of CDK1. Although there was no discernible phenotypic change in CDK2, higher levels of the protein were detected in E6 cells. In accordance with the CDK2 activity measurements (Fig. 3C), cyclin A, which is the main partner of CDK2 in the G2 to M phase [14,25], began to disappear at 9 h.

The kinetics of cyclin B1 production was strikingly different between A549-neo and A549-E6 cells. Cyclin B1 was detected in A549-neo cells for the first 6 h, but quickly disappeared thereafter. In contrast, we detected a strong signal for cyclin B1 in A549-E6 cells for at least 15 h after the addition of caffeine, although the signal was weaker at 12 and 15 h than at 9 h. These differences in cyclin B1 signal strength, in combination with the

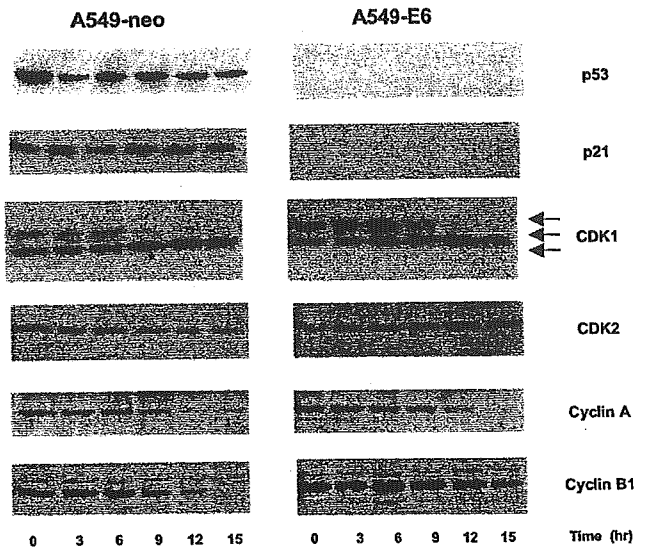

Fig. 4. Western blotting analysis of proteins that are associated with CDK1 and CDK2 activities. Cell extracts of G2-arrested A549-neo and A549-E6 cells were prepared at 3-h intervals after treatment with caffeine. Aliquots (25 μg) of the proteins were separated on SDS–polyacrylamide gel electrophoresis and blotted onto a nitrocellulose filter. The filters were then probed with antibodies and the signals were detected as described under Materials and methods.

band-shift profiles of CDK1 in both cell lines, can explain the observed cell morphologies and CDK1 activities shown in Figs. 2A and 3A, respectively. Thus, the slower rate of traverse of mitosis in A549-E6 cells might be interpreted as a failure to achieve efficient inactivation of CDK1 due to inefficient degradation of cyclin B1.

Degradation of cyclin B1 and completion of M phase after butyrolactone I treatment

We examined the causal relationship between high CDK1 activity/stable cyclin B1 and slower traverse of the M phase in A549-E6 cells. We studied the effect of butyrolactone I, which is a specific inhibitor of CDK1 and CDK2 [26], on the M phase of A549-E6 cells. The rationale behind this experiment evolved from evidence that inhibition of CDC28 kinase activity by the CDK inhibitor Sic1 of *Saccharomyces cerevisiae* plays a central role in triggering the completion of M phase [27–29].

The addition of butyrolactone I to rounded A549-E6 cells 12 h after caffeine treatment (Fig. 5A; left panel) induced a remarkable reduction in the number of floating round cells in the culture. Instead, there was an obvious increase in the number of adherent cells, compared with non-treated cells, after 3 h (right panel in Fig. 5A). These results suggest that butyrolactone I inhibits CDK1 activity, which in turn induces M-phase exit. In order to confirm this result biochemically, CDK1 activity was measured. CDK1 activity was depressed in butyrolactone I-treated cells compared with nontreated

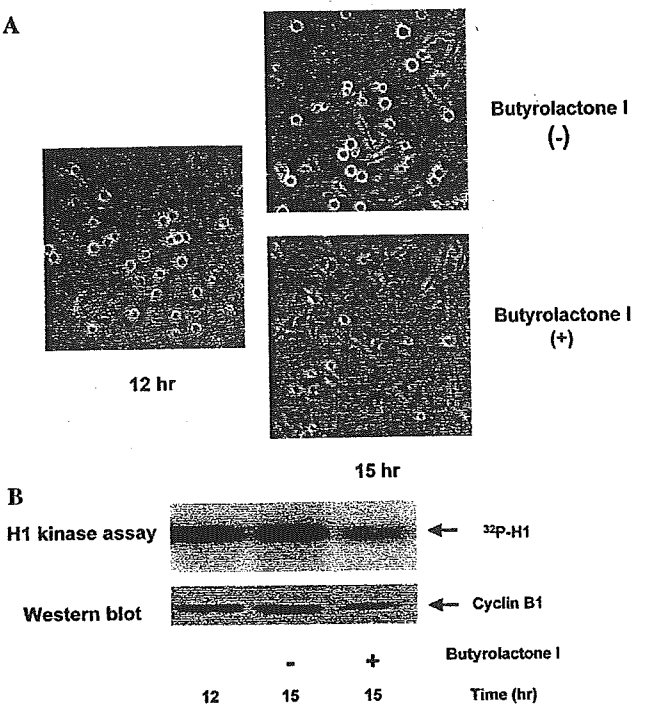

Fig. 5. The effects of butyrolactone I on caffeine-treated A549-E6 cells. (A) A549-E6 cells that were treated with 2.5 mM caffeine for 12 h appear as rounded cells (left panel). These cells were subsequently incubated in the absence (upper right panel) or presence (lower right panel) of 25 μM butyrolactone I for an additional 3-h period. The micrographs were taken under phase contrast. (B) CDK1 kinase activities on histone H1 at the time points described in A are shown in the upper panel. A Western blot of cyclin B1 is shown in the lower panel. Butyrolactone I at 25 μM for 24 h induced both G1 and G2 arrest in A549-neo and -E6 cells as reported for other cells ([31]; data not shown).

cells (Fig. 5B). Buffer-washed immunoprecipitates of CDK1 that were pretreated with butyrolactone I were previously shown to be active [30]. Therefore, the differences in CDK1 activity between the samples in Fig. 5B should reflect the kinase activities of these cells.

The levels of cyclin B1 in butyrolactone I-treated and nontreated cells were determined by Western blotting. Interestingly, significantly lower amounts of cyclin B1 were detected in butyrolactone I-treated cells than in nontreated cells. Taken together, butyrolactone I administration to caffeine-treated rounded cells induces M-phase exit, which is accompanied by the disappearance of cyclin B1 and the inactivation of CDK1.

In summary, we described a notable change in the cell lines with or without E6 oncogenes of HPV16 after the G2 checkpoint was abrogated. The progression of p53-inactive A549-E6 cells to the M phase was slowed significantly compared to the parental cells, and this slowing was accompanied by high levels of CDK1 activity. Our results strongly suggest that the high CDK1 activity levels in A549-E6 cells that prevent exit to the M phase are due to mechanisms that prevent the degradation of cyclin B1, since reasonably high levels of cyclin

B1 were detected in our experiments. This notion is supported by evidence from experiments with the CDK inhibitor butyrolactone I, in which cyclin B1 degradation and morphological changes were induced. A549-neo cells traverse quickly to the M phase, even though the rate of traverse is slower than that seen during a normal cell cycle. It should be noted that we cannot conclude that the abrogation of p53 always results in the retarded progression of M phase since we have not analyzed other p53-positive cell lines. Even if so, our results can at least partially explain why cell lines without functional p53 usually exhibit mitotic catastrophe to die when the G2 checkpoint is abrogated.

Finally, the observations presented in this report suggest a link between the p53 pathway that is activated by DNA damage and the M-phase traverse, especially in ubiquitin-dependent degradation of cyclin B1 to exit mitosis. Although the loss of p53 induces many effects on cell cycle progression by controlling gene expression, taking into account that attenuation of CDK1 activity is critical in the degradation of cyclin B, the $p21^{Cip1}$ gene is one of the strongest candidate genes that can attenuate CDK1 activity in the situation here. Our results using butyrolactone I allow us to argue that p21 has some important role in the inactivation of CDK1 during mitosis in G2-checkpoint-abrogated cells, and this triggers the disintegration of cyclin B1 and the exit of cells from the M phase. Further experiments, such as the direct delivery of p21 protein to G2-checkpoint-abrogated p21-null cells, are needed to evaluate the precise contribution of the gene, and are now in progress.

Acknowledgments

We thank Dr. Touho Yoshida (Institute for Fermentation, Osaka, Japan) for providing A549 cells. We also thank Drs. Masuo Yutsudo (Osaka University, Japan) and Bert Vogelstein (Johns Hopkins University, USA) for generous gifts of plasmids. This work was supported in part by Grants-in-Aid for Scientific Research (to Y.I.) and for the Second Term of the Comprehensive 10-Year Strategy for Cancer Control (to H.N.) from the Ministry of Health, Labor, and Welfare of Japan.

References

[1] M.B. Kastan, Q. Zhan, W.S. El-Deiry, F. Carrier, T. Jacks, W.V. Walsh, B.S. Plunkett, B. Vogelstein, A.J. Fornance Jr., Cell 71 (1992) 587–597.
[2] Q. Zhan, F. Carrier, A.J. Fornance Jr., Mol. Cell. Biol. 13 (1993) 4242–4250.
[3] X.W. Wang, H. Yeh, L. Schaeffer, R. Roy, V. Moncollin, J.M. Eagly, Z. Wang, E.C. Friedberg, M.K. Evans, B.G. Taffe, C.C. Harris, Nature Genet. 10 (1995) 188–195.
[4] S. Bates, K.H. Vousden, Curr. Opin. Genet. Dev. 6 (1996) 12–18.
[5] A.J. Levine, Cell 88 (1997) 323–331.
[6] M.S. Greenblatt, W.P. Bennett, M. Hollstein, C.C. Harris, Cancer Res. 54 (1994) 4855–4878.
[7] L.J. Ko, C. Prives, Genes Dev. 10 (1996) 1054–1072.
[8] M.L. Agarwal, A. Agarwal, W.R. Taylor, G.R. Stark, Proc. Natl. Acad. Sci. USA 92 (1995) 8493–8497.
[9] Z.E. Winters, W.M. Ongkeko, A.L. Harris, C.J. Norbury, Oncogene 17 (1998) 673–684.
[10] T.M. Passalaris, J.A. Benanti, L. Gewin, T. Kiyono, D.A. Galloway, Mol. Cell. Biol. 19 (1999) 5872–5881.
[11] S. Dan, T. Yamori, Biochem. Biophys. Res. Commun. 280 (2001) 861–867.
[12] Y. Zhou, G. Gwadry, W.C. Reinhold, L.D. Miller, L.D. Smith, U. Scherf, E.T. Liu, K.W. Kohn, Y. Pommier, J.N. Weinstein, Cancer Res. 62 (2002) 1688–1695.
[13] W.R. Taylor, G.R. Stark, Oncogene 20 (2001) 1803–1815.
[14] Y. Minemoto, J. Gannon, M. Masutani, H. Nakagama, T. Sasagawa, M. Inoue, Y. Masamune, K. Yamashita, Exp. Cell Res. 262 (2001) 37–48.
[15] M. Yutsudo, Y. Okamoto, A. Hakura, Virology 166 (1988) 594–597.
[16] S.E. Kern, J.A. Pietenpol, S. Thiagalingam, A. Seymour, K.W. Kinzler, B. Vogelstein, Science 256 (1992) 827–830.
[17] W.S. El-Deiry, T. Tokino, V.E. Velculescu, D.B. Levy, R. Parsons, J.M. Trent, D. Lin, W.E. Mercer, K.W. Kinzler, B. Vogelstein, Cell 75 (1993) 817–825.
[18] A. Koff, A. Giordano, D. Desai, K. Yamashita, J.W. Harper, S.J. Elledge, T. Nishimoto, D.O. Morgan, B.G. Franza, J.M. Roberts, Science 257 (1992) 1689–1694.
[19] K. Yamashita, H. Yasuda, J. Pines, K. Yasumoto, H. Nishitani, M. Ohtsubo, T. Hunter, T. Sugimura, T. Nishimoto, EMBO J. 9 (1990) 4331–4338.
[20] T.D Kessis, R.J. Slebos, W.G. Nelson, M.B. Kastan, B.S. Plunkett, S.M. Han, A.T. Lorincz, L. Hendrick, K.R. Cho, Proc. Natl. Acad. Sci. USA 90 (1993) 3988–3992.
[21] J.W. Harper, G.R. Adami, N. Wei, K. Keyomarsi, S.J. Elledge, Cell 75 (1993) 805–816.
[22] S.L. Yao, A.J. Akhtar, K.A. McKenna, G.C. Bedi, D. Sidransky, M. Mabry, R. Ravi, M.I. Collector, R.J. Jones, S.J. Sharkis, E.J. Fucks, A. Bedi, Nat. Med. 2 (1996) 1140–1143.
[23] C.A. Hall-Jackson, D.A. Cross, N. Morrice, C. Smythe, Oncogene 18 (1999) 6707–6713.
[24] J.N. Sarkaria, E.C. Busby, R.S. Tibbetts, P. Roos, Y. Taya, L.M. Karnitz, R.T. Abraham, Cancer Res. 59 (1999) 4375–4382.
[25] N. Furuno, N. Elzen, J. Pines, J. Cell Biol. 147 (1999) 295–306.
[26] M. Kitagawa, T. Okabe, H. Ogino, H. Matumoto, I. Suzuki-Takahashi, T. Kokubo, H. Higashi, S. Saitoh, Y. Taya, H. Yasuda, Y. Ohba, S. Nishimura, N. Tanaka, A. Okuyama, Oncogene 8 (1993) 2425–2432.
[27] T.T. Nugroho, M.D. Mendenhall, Mol. Cell. Biol. 14 (1994) 3320–3328.
[28] R. Visintin, K. Craig, E.S. Hwang, S. Prinz, M. Tyers, A. Amon, Mol. Cell 2 (1998) 709–718.
[29] M. Shirayama, A. Toth, M. Galova, K. Nasmyth, Nature 402 (1999) 203–207.
[30] R.Y. Poon, M.S. Chau, K. Yamashita, T. Hunter, Cancer Res. 57 (1997) 5168–5178.
[31] M. Kitagawa, H. Higashi, I.S. Takahashi, T. Okabe, H. Ogino, Y. Taya, S. Nishimura, A. Okuyama, Oncogene 9 (1994) 2549–2557.